

type of argument applied to the other states considered in Secs. III and IV.

(d) Conclusions

Singlet and triplet S , even $P(L_z=0)$, Σ_g^+ , Σ_g^- projections of a two electron UPSD have been studied in detail. The most general correspondence between an UPSD and a MWF with arbitrary linear coefficients has been shown to be given by Eqs. (40) and (50), and the quantitative implications are discussed in Secs. (Va) and (Vb). The conditions for the applicability of the generalized Koopmans' theorem are discussed (Sec. Vc) and it is shown that for a sufficiently unrestricted projected two-electron Slater determinant

there is no two-dimensional Fock-Dirac fundamental invariant.

The handling of many-particle operators of the type $\mathcal{H}\mathcal{O}$ offers little hope, at least with present day electronic computers. Further advance in this area requires the evaluation of the second order density matrix corresponding to $\Psi = \mathcal{O}D$, which we attempted unsuccessfully.

ACKNOWLEDGMENTS

I am indebted to my wife Annik for help in the preparation of this paper, as well as to many members of the Quantum Theory Project for their kind encouragement, especially to Professor Darwin W. Smith for valuable comments on the final manuscript.

Measurement of Charge-Exchange Cross Sections for H^+ , H_2^+ , and He^+ Ions*

DAVID W. KOOPMAN

University of Maryland, College Park, Maryland

(Received 20 June 1966; revised manuscript received 12 October 1966)

Measurements have been made of the charge-exchange cross sections for the ion-molecule pairs: $H^+ + H_2$, $H_2^+ + H_2$, $H^+ + Ar$, $H_2^+ + Ar$, $H^+ + Kr$, $H_2^+ + Kr$, $H^+ + Xe$, $H_2^+ + Xe$, $He^+ + Ar$, $He^+ + Kr$, and $He^+ + Xe$ in the energy range of 70 to 1050 eV, employing electric fields in a collision chamber to collect slow ion-collision products. The present work generally confirms previous measurements, but shows larger values for low-energy cross sections of Kr and Xe, a systematic discrepancy that can be attributed to the design of the apparatus used in previous work. The present results are consistent with the predictions of the adiabatic theory and with reported observations of optical excitation of the heavy rare gases by low-energy helium-ion charge-exchange processes.

INTRODUCTION

COLLISION cross sections for various atomic processes are of importance in determining the composition and behavior of plasmas occurring both naturally and in laboratory experiments and are valuable in verifying and guiding the theoretical treatment of atomic interactions. In the present investigations, measurements have been made of charge-exchange cross sections for reactions of the type $A^+ + B \rightarrow A + B^+$, where the incident ions consisted of the species H^+ , H_2^+ , or He^+ and the neutral target molecules examined were H_2 , Ar, Kr, and Xe. Although the relative simplicity of the ions and gases studied might suggest that definitive calculations or measurements of the charge-exchange cross sections for these species have already been made, a review of some of the more recent literature discloses that considerable uncertainty still remains, particularly

for ion energies below 300 eV and for the heavier rare gases.¹⁻⁹

A more exact knowledge of these cross sections would, in particular, serve to examine the general applicability of the adiabatic theory,¹⁰ which predicts a maximum cross section when the velocity v of the incident ion satisfies the condition

$$v = a|\Delta E|/h, \quad (1)$$

where a is a distance of the order of 5 to 10 Å and ΔE

¹ F. Wolf, *Ann. Physik* **30**, 313 (1937).

² J. B. Hasted, *Proc. Roy. Soc. (London)* **A205**, 421 (1951).

³ J. B. H. Stedeford and J. B. Hasted, *Proc. Roy. Soc. (London)* **A227**, 406 (1955).

⁴ H. B. Gilbody and J. B. Hasted, *Proc. Roy. Soc. (London)* **A238**, 334 (1956).

⁵ D. P. Sural and N. C. Sil, *J. Chem. Phys.* **42**, 729 (1965).

⁶ W. H. Cramer, *J. Chem. Phys.* **35**, 836 (1966).

⁷ D. W. Vance and T. L. Bailey, *J. Chem. Phys.* **44**, 486 (1966).

⁸ M. G. Menendez, B. S. Thomas, and T. L. Bailey, *J. Chem. Phys.* **42**, 802 (1965).

⁹ E. Lindholm, *Arkiv Fysik* **18**, 219 (1960).

¹⁰ H. S. W. Massey and E. H. S. Burhop, *Electronic and Ionic Impact Phenomena*, (Oxford University Press, New York, 1952), p. 450.

* This work was supported by the Office of Space Science and Applications, National Aeronautics and Space Administration, under Grant NsG-283-62.

is the effective energy difference between the initial and final states of the joint atomic system. ΔE is commonly computed for the type of process considered in this investigation from the expression

$$\Delta E = \Delta(IP) + \bar{E}_p + E_{\text{excit}},$$

where $\Delta(IP)$ is the difference of the ionization potentials of the neutral species, \bar{E}_p is an average polarization term which can be approximated by a procedure given by Hasted and Lee,¹¹ and E_{excit} is the energy represented by the participation of excited states in the collision process. When ΔE is small, particularly when a symmetric process of the type $A^+ + A \rightarrow A + A^+$ is considered, the cross section is expected to be large at low ion velocities, falling as the incident ion velocity is increased. Such a cross-section dependence is said to be of resonance form. Appreciable values for ΔE generally lead to cross sections that are small at low velocities and have maxima at velocities given by (1); such cross sections are termed to be of defect form. The adiabatic theory has been successful in predicting the location of cross-section maxima for a large number of collision processes; its application to the reactions studied in the present investigation is described in greater detail below.

APPARATUS

A schematic diagram of the apparatus used in the present investigation is shown in Fig. 1. Hydrogen or helium gas was admitted to an Ortec Model 320 radio-frequency ion source through an electrically controlled leak valve. Extraction and acceleration electrodes at the exit from the source directed the ion beam into a 127° electrostatic energy analyzer.¹² The midline of the analyzer plates had a radius of 10.16 cm and the plate separation was 2.54 cm, so that voltages $\pm V_0$

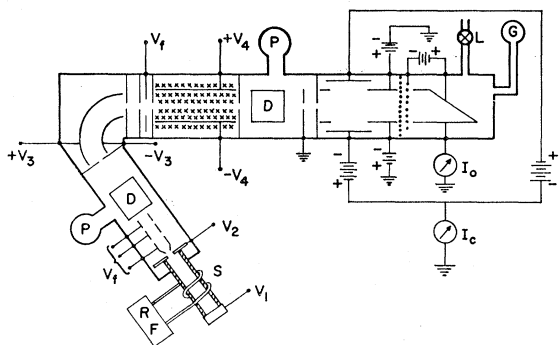


FIG. 1. Diagram of apparatus (not to scale). *RF*, radio frequency oscillator; *S*, ion source; V_1 , acceleration voltage; V_2 , extraction voltage; V_3 , focusing voltages; V_3 , energy analyzer; V_4 , velocity selector voltage; *P*, vacuum pumps; *D*, deflection plates; *L*, gas inlet; *G*, pressure gauges.

¹¹ J. B. Hasted and A. R. Lee, Proc. Phys. Soc. (London) **79**, 702 (1962).

¹² A. L. Hughes and V. Rojansky, Phys. Rev. **34**, 284 (1929).

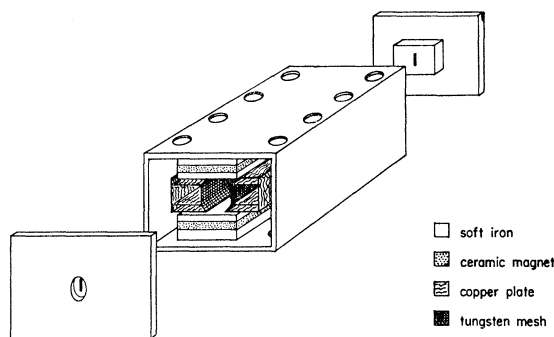


FIG. 2. Diagram of velocity selector interior, showing shape of electric field plates and end configuration.

applied to the plates refocused ions with energy per unit charge of $4V_0$ at the output slit. Slit widths were chosen so that the energy spread of the ion beam emerging from the analyzer was approximately $\pm 4\%$. A portion of the outer plate was constructed as a grid to allow neutral beam components to escape without being deposited on the electrode surface.

The selection of the desired species from the monoenergetic beam emerging from the energy analyzer was performed by a crossed field velocity selector,¹³ within which a 250-G vertical magnetic field was supplied by permanent ceramic magnets fitted with soft iron pole pieces measuring 10 cm \times 5 cm and separated by 2.54 cm. The variable transverse electric field was established between tungsten mesh electrodes separated by 2.5 cm on the axis and supported by box-like structures which trapped those ions separated from the beam. Surrounding the velocity selector was a soft iron housing which served as a return yoke for the magnetic field and which confined the field to the interior of the selector. The condition for undeflected passage of an ion species is given by $\mathbf{F}_e = \mathbf{F}_B$ or $e\mathbf{E} = e(\mathbf{v} \times \mathbf{B})/c$, where \mathbf{F}_e and \mathbf{F}_B are the transverse electric and magnetic forces, \mathbf{E} is the transverse electric field strength, \mathbf{B} is the magnetic field strength, e is the ionic charge, and \mathbf{v} is the velocity; the vital condition for satisfactory operation of the selector is that the ratio of the perpendicular components of \mathbf{E} and \mathbf{B} be constant along the region near the beam axis. To satisfy this condition, the electric plates were shaped to yield a more nearly uniform field that flat plates would produce. Moreover, to achieve proportional, although not necessarily uniform, \mathbf{B} and \mathbf{E} fields at the ends of the selector, the shape of the end plates carrying the slits was chosen so that the electric field, as governed by the Laplace equation, and the magnetic field, as governed by the magnetostatic analog of the Laplace equation (valid for the high μ pole pieces and end plates) would have the same spatial dependence. A diagram of the selector design is shown in Fig. 2 and the voltage-energy relation obtained is shown in Fig. 3.

¹³ W. Bleakney and J. A. Hipple, Phys. Rev. **53**, 521 (1938).

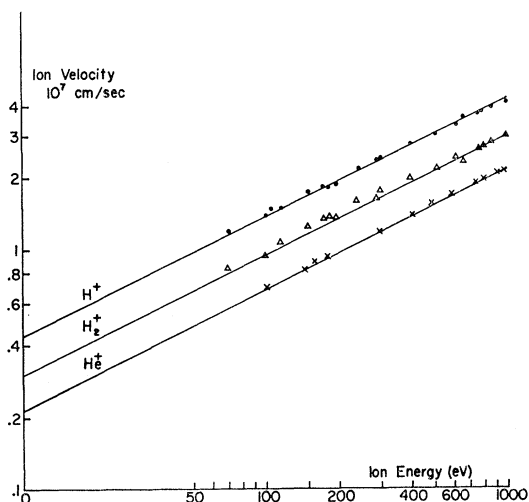


FIG. 3. Velocity calculated from applied electric field versus measured ion energy for H^+ , H_2^+ , and He^+ ions passing through velocity selector.

The beam emerging from the velocity selector was directed into the collision chamber, in which nearly uniform electric fields perpendicular to the beam axis were used to separate the slow charged species produced by collisions from the primary beam. Guard plates with apertures surrounded the electrodes collecting the slow ions and electrons for measurement. The guard plates were 1.45 cm apart, with apertures 1 cm square. The front edges of the apertures were 0.5 cm from the collision-chamber entrance and the rear edges were 0.5 cm from the entrance to a Faraday cup. The collecting plates were 0.3 cm beyond the apertures. By reading the net current to both the positive and negative collection plates, compensation for ionization processes in the gas and secondary electron emission at the negative electrode was achieved. At the rear of the collision chamber a Faraday cup covered by two 95% transparency grids collected the primary beam. The first grid was grounded; the second grid was biased 15 V negative with respect to the cup to suppress secondary electron effects which otherwise both increased the apparent primary current and caused a large negative scattered current at the collection plates. Currents to the collection plates and to the Faraday cup were measured on Keithley Model 610B electrometers.

The system was evacuated by two oil diffusion pumps to a pressure of approximately 10^{-6} Torr before experimental measurements were made. Research-grade gases, with less than a few parts per million impurity levels, were admitted to the collision chamber through a mechanical leak valve, and could escape only through the 0.05 cm^2 hole through which the primary beam passed. To measure the gas pressure within the chamber, a Varian mTorr ionization gauge, with a linear response between pressures of 5×10^{-5} and 1×10^{-1} Torr,

was used. To obtain the factor required to convert the ionization gauge readings into pressures for the various gases, the ionization gauge was calibrated against an MKS Instruments Baratron absolute capacitance manometer. As shown in Fig. 4, a linear relation was confirmed, and conversion factors accurate to $\pm 5\%$ were obtained. An article discussing the accuracy of a similar high-sensitivity capacitance manometer has recently been published.¹⁴

To measure the true energy of the ions comprising the primary beam, the second grid of the Faraday cup could alternatively be connected to an external voltage source. The positive retarding potential necessary to reduce the primary current by one-half was taken as the beam energy. It was determined that this procedure was more accurate than relying on the energy-analyzer plate voltages which, because of minor aberrations in the ion optics, were not strictly proportional to the beam energy. Typical blocking potential-primary current relationships are shown in Fig. 5.

To check that some process other than charge exchange was not enhancing the cross section measured, studies were made of the separate currents to the positive and negative collection plates in the collision chamber as the collecting field was varied from zero to its maximum value. It was found that fields of less than 0.5 V/cm were sufficient to prevent any of the pressure-dependent positive current observed at zero collection field from reaching the positive collection plate, ensuring that elastic scattering of the main beam, photon processes, etc., were not responsible for a significant fraction of the collected current. The collected negative current was found to vary little with either gas pressure or collection field, indicating that cross sections for

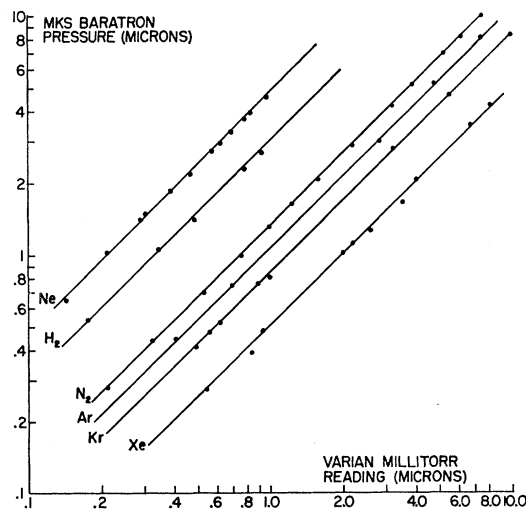


FIG. 4. Measured relationships between pressure readings from Varian ionization gauge and Baratron capacitance manometer.

¹⁴ N. G. Utterbeck and T. Griffith, Jr., *Rev. Sci. Instr.* **37**, 866 (1966).

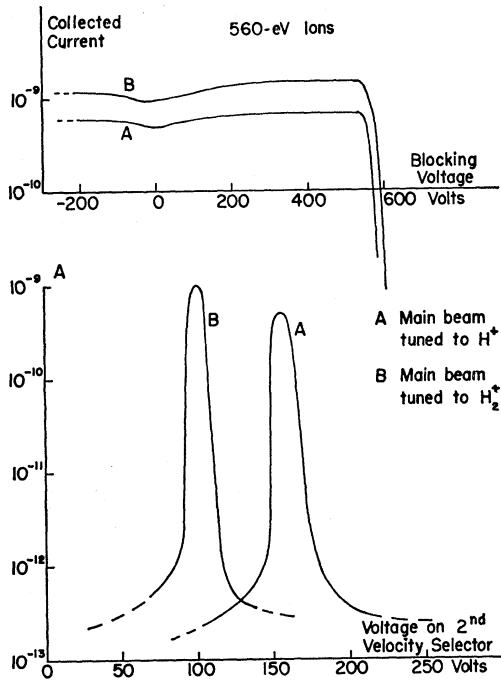


FIG. 5 (a) Collected current versus retarding potential applied to Faraday cup grid; (b) output current of second velocity selector versus voltage applied to second velocity selector plates, indicating purity of the primary beam.

ionization processes were small ($\leq 10\%$) compared to the charge-exchange reactions studied. The leakage current to the collection plates, due to imperfect insulation of the circuit, was typically -5×10^{-13} A and was independent of collision chamber pressure and unaffected by pressure-gauge operation.

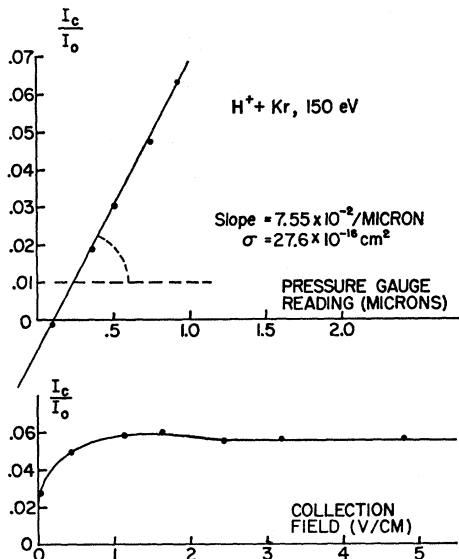


FIG. 6. (a) Dependence of collected current ratio on pressure of gas in collision chamber; (b) dependence of collected current ratio on collecting field strength.

For the various ion species and gases studied, the dependence of the net collected current on collecting field was determined. A typical relation is shown in Fig. 6(b), where a saturation is observed for fields above 2 V/cm. All cross-section measurements were performed using a collection field adequate to ensure saturation.

To verify that the apparatus was delivering a single-ion species to the collision chamber, the collision chamber was temporarily replaced by a second velocity selector, followed by a grid-covered Faraday cup. When the ion beam was established, the current to the Faraday cup was recorded as the voltage across the second velocity selector was varied. The results of such a study are shown in Fig. 5(b). It was determined that the primary beam consisted of the single species expected with a purity of better than 99.5% for energies above 150 eV; for lower energies, purities of at least 98% were typical.

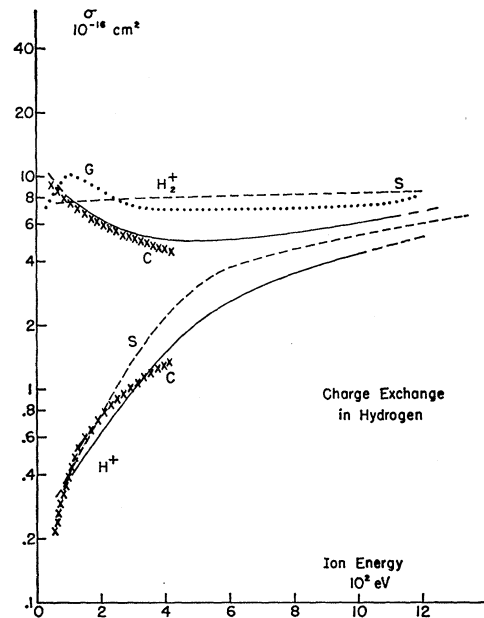


FIG. 7. Charge-exchange cross sections for H⁺ and H₂⁺ in hydrogen. Solid curve, present work; S, Stedford and Hasted; G, Gilbody and Hasted; C, Cramer.

EXPERIMENTAL PROCEDURE AND DATA REDUCTION

The procedure used in performing the measurements was as follows: The ion current for the desired species was established and the energy was measured by applying the retarding potential to the Faraday cup grid. The voltage on the velocity selector plates was also recorded. The primary current was typically in the range 5×10^{-11} to 5×10^{-8} A. The primary current I_0^* , the collected current I_c^* , and the pressure gauge reading p^* were recorded as the gas pressure was increased above its minimum value of 2×10^{-5} Torr. By limiting

the maximum gas pressure, the collected current was held to only a few percent of the primary current value. For each energy examined, between 5 and 15 separate pressure values were used. In the absence of the ion beam, the leakage current to the collection plates, I_L , was also measured; the leakage current to the Faraday cup was negligible. At the end of an experimental run, the ionization gauge was recalibrated against the capacitance manometer. Figure 6(a) shows the dependence of collected current on pressure for a particular experimental measurement; the negative current at the lowest pressure represents residual secondary-electron emission by the primary beam at the Faraday cup surfaces.

The data were reduced to punch card form and processed on the University 7090 computer by a

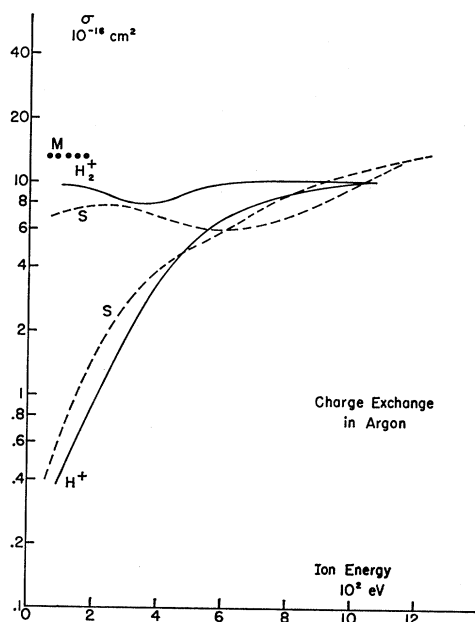


FIG. 8. Charge-exchange cross sections for H^+ and H_2^+ in argon. Solid curve, present work; S, Stedford and Hasted; M, Menendez *et al.*

program written in the Michigan Algorithm Decoder (MAD) language for this purpose. Spot checks were also made by hand calculation. In the reduction procedure, the collected current was corrected for the leakage to obtain the true collected current $I_c = I_c^* - I_L$; the losses in the primary beam between the collection region and the Faraday cup were approximately corrected to obtain the true primary current $I_0 = I_0^* + I_c^* - I_L$. In the machine calculation, a least-squares linear fit between the quantities I_c/I_0 and p^* was performed; the slope obtained was converted through knowledge of the collection length l and the conversion factor between the true pressure p and the pressure gauge reading p^* to obtain the cross section σ through the relation $I_c/I_0 = lN\sigma$, where N is the gas molecular number

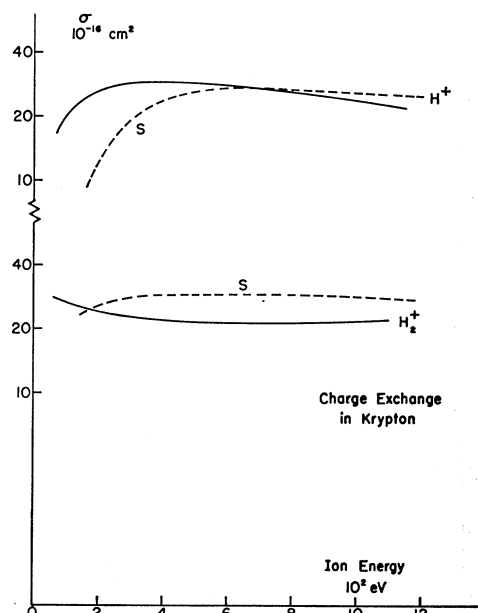


FIG. 9. Charge-exchange cross sections for H^+ and H_2^+ in krypton. Solid curve, present work; S, Stedford and Hasted.

density at pressure p . Also included in the computer output for each measurement were a parameter based on the mean-square deviation of data points about the linear relationship and a value for the ion mass calculated from the energy and velocity selector voltage. Cross-section values for which the scatter parameter was large or for which the computed ion mass was significantly different from the expected value were discarded.

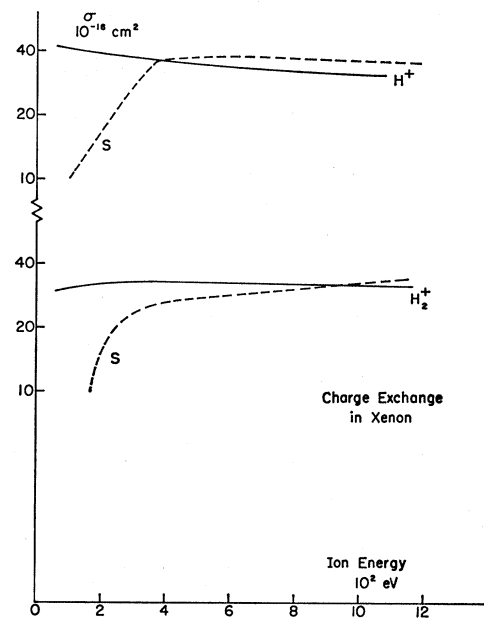


FIG. 10. Charge-exchange cross sections for H^+ and H_2^+ in xenon. Solid curve, present work; S, Stedford and Hasted.

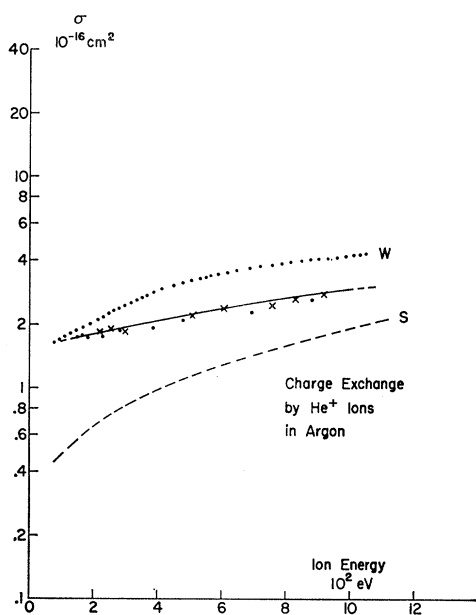


FIG. 11. Charge-exchange cross section for He^+ in argon. Solid curve, present work; W, Wolf; S, Stedeford and Hasted.

For each process investigated, separate measurements at energies between 70 and 1050 eV were made on different days, with separate pressure calibrations on each day. The results presented in this paper represent measurements which were in agreement to within the random scatter on two or more days; the random scatter was approximately $\pm 10\%$, except for cross sections below 10^{-16} cm^2 or for ion energies below 150 eV, where $\pm 20\%$ reproducibility was typical. The absolute accuracy was governed mainly by uncertainties in the pressure calibration and the slow ion collection efficiency, estimated to be $\pm 5\%$ and $\pm 15\%$, respectively.

RESULTS AND CONCLUSIONS

Figures 7 through 12 present the values for the charge-exchange cross sections measured in this investigation; the results of some previous studies are also given. In general it can be seen that the measured cross sections agree fairly well with previous results, except for the low-energy range in the heavy rare gases. For these gases, the values now are found to have a nearly constant value down to the lowest energies examined.

The reactions $\text{H}^+ + \text{H}_2 \rightarrow \text{H} + \text{H}_2^+$ and $\text{H}_2^+ + \text{H}_2 \rightarrow \text{H}_2 + \text{H}_2^+$ are of particular interest because of the relative simplicity of the atomic systems involved and because of the numerous previous studies. The present work is in close agreement with the results of Cramer,⁶ which were made with an apparatus specifically designed to examine low energies. The increase of the $\text{H}_2^+ + \text{H}_2$ cross section below 500 eV was previously observed down to 200 eV by Gilbody and Hasted⁴ below which energy an apparent decrease was found. The

present study tends to confirm the steady increase to energies below 100 eV, as would be expected for a resonant process. The values obtained for the process $\text{H}_2^+ + \text{Ar} \rightarrow \text{H}_2 + \text{Ar}^+$ by Menendez *et al.*⁸ at energies below 150 eV are about 30% higher than the present results but do not indicate the downward trend reported by Stedeford and Hasted.³

It is this last reference that is the source of previous values for the charge-exchange process with Kr and Xe, with which the present results differ most significantly, so it is of particular importance to indicate the features of the two experiments which might account for the discrepancy. The previous experiment was done with the same magnetic field which analyzed the ion beam acting on the collision chamber parallel to the collecting electric fields and assisting in controlling and collecting the slow ions produced by charge-exchange reactions. As Hasted pointed out,³ if the radii of ion paths in the field were not small compared to the collection apertures, the magnetic field could not dependably control the collected ions. This criterion was difficult to meet for heavy ions, even if only thermal energies were considered. In addition, however, the previous studies employed a fixed, high ion energy for beam analysis (so that a large magnetic field could be used) with a deceleration of the beam at the entrance to the collision chamber. Experience in field mapping and in acceleration and deceleration of ion beams in the author's laboratory has emphasized the surprising penetration of strong fields through slits and apertures. Therefore, in the earlier studies, the growth of a penetrating fringe of the decelerating field at progressively lower energies may have been responsible for systematic loss of

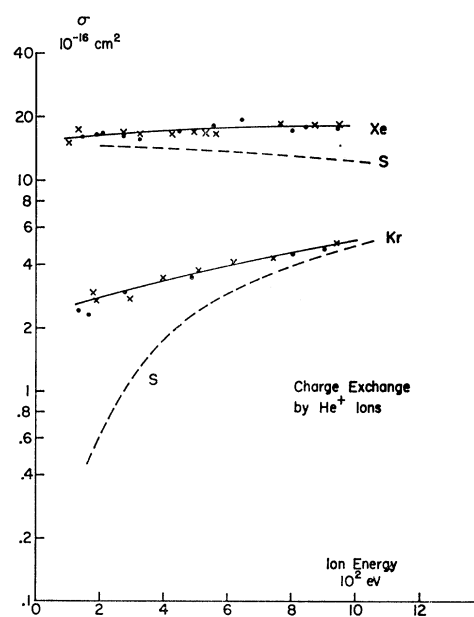


FIG. 12. Charge-exchange cross sections for He^+ ions in krypton and xenon. Solid curve present work; S, Stedeford and Hasted.

collected currents of heavy ions. The present experiment, by contrast, employs no deceleration at the collision chamber with attendant field-penetration problems, and because the collection of collision products is controlled only by electrostatic fields, no systematic change of collection efficiency with ion mass should occur.

A possible difficulty in comparing the present results for H_2^+ ions to those of previous investigators is the unknown concentration of excited ions in the primary beam. In the results for Kr and Xe, however, the relative differences between the present values and those of Hasted and Stedeford are approximately the same for H_2^+ ions as for H^+ ions, where the excitation difficulty does not arise. For the lighter target gases, present results are in substantial agreement with earlier measurements with H_2^+ ions, further indicating that the excitation problem is no greater in the present work, which employed an rf ion source, than in earlier studies, where electron bombardment sources were generally used.

The values for the charge-exchange cross sections of He^+ ions with the rare gases Ar, Kr, and Xe are found to be fairly constant down to the lowest energies examined, the dependence for Kr being most different from that obtained by Hasted. If the quantity $|\Delta E|$ is calculated for these reactions, neglecting the possibility of excited states in the rare-gas ions, cross-section maxima at energies in the range of 10^4 to 10^5 eV are predicted by (1), because of the large difference between the ionization potentials of helium and the heavy rare gases. It can be concluded that the large and nearly constant cross-section values observed at low energies are indications of the excitation of the slow ions. The present work is accordingly a direct confirmation of a postulated explanation of large optical excitation cross sections for heavy rare gases bombarded by slow helium ions, as reported by Lipeles, Novick, and Tolk,¹⁵ who attributed the observed Ar^+ , Kr^+ , and Xe^+ line emission to a de-excitation of excited rare-gas ions created by a charge-exchange process. The reader is referred to their paper for detailed energy level diagrams which demonstrate an extremely small $|\Delta E|$ for these processes, if excited states are considered.

The comparison of the present results to the predictions of the adiabatic theory is somewhat confused by the strong influence of polarizability terms on the value for $|\Delta E|$ for the heavy rare gases. Hasted and Lee have

evaluated an integral of the form

$$\bar{E}_p = \frac{\int \int E_p db dx}{\int \int db dx}$$

between limits r_1 and r_2 , where r_1 is the maximum inter-nuclear separation at which reactions will take place, and r_2 is the minimum separation of importance in collisions of the type considered here; the value for E_p is found to be approximately proportional to $(r_1^3 r_2)^{-1}$. In choosing the value for r_1 , they were led by scaled wave-function arguments to adopt values of approximately 2 Å. It would appear, however, from consideration of the maximum cross sections (as large as 40 Å) and from the apparent invariance of the quantity a that a value of perhaps 3.5 Å would be a more realistic estimate for r_1 . Using this modification in the calculation of the effective energy defect, together with the ion energy value V_m at which cross section maxima occur, the quantity a has been calculated from (1), rewritten in the form $a = h(2V_m/m)^{1/2} |\Delta E|^{-1}$, where m is the mass of the incident ion. The results are presented in Table I,

TABLE I. Values of a calculated from experimental data.

Process	Reference	$(V_m)^{1/2}$ (eV ^{1/2})	ΔE (eV)	a (Å)
$H^+ + He$	2	160	10.48	8.5
$H^+ + Ne$	2	80	-7.73	6.0
$H^+ + Ar$	2	40	-2.63	8.8
$H^+ + Kr$	present	17	-1.38	7.15
$H^+ + Xe$	present	<10	-0.13	<45*
$H_2^+ + Ne$	2	150	-5.79	10.6
$H_2^+ + Ar$	present	<10	-0.71	≤5.8
$H_2^+ + Kr$	present	≤10	+0.54	≤7.8
$H_2^+ + Xe$	present	18.8	+1.77	4.4
$He^+ + Ne$	2	80	3.17	7.2
$He^+ + Ar$	2	200	10.0	5.6

* This result is very sensitive to the polarization-energy approximation, because the sign of energy defect is apparently reversed.

where it is apparent that the values obtained for a lie in the expected range of 5 to 10 Å for most of the cases considered.

ACKNOWLEDGMENTS

The author would like to thank Dr. T. D. Wilkerson for his support and advice during the course of this investigation. The assistance of P. G. Cable and M. Kato in development of the vacuum system and apparatus is also gratefully appreciated.

Computing facilities were provided by the University of Maryland Computer Science Center.

¹⁵ M. Lipeles, R. Novick, and N. Tolk, Phys. Rev. Letters **15**, 815 (1965).